

論文 / 著書情報
Article / Book Information

論題(和文)	
Title(English)	Global Behavior of Viscoelastic Damper based on Heat Flow Characteristics
著者(和文)	Osabel Dave, 笠井 和彦, 佐藤大樹
Authors(English)	Dave M Osabel, Kazuhiko Kasai, Daiki Sato
出典(和文)	日本建築学会大会学術講演梗概集, , , pp. 569-570
Citation(English)	, , , pp. 569-570
発行日 / Pub. date	2022, 9
権利情報	一般社団法人 日本建築学会

Global Behavior of Viscoelastic Damper based on Heat Flow Characteristics

正会員 ○OSABEL Dave M.*1 同 笠井 和彦*2 同 佐藤 大樹*3

Viscoelastic Damper
Heat Transfer Analysis

Dynamic Behavior

Long-duration Loading

3D Finite Element Analysis

1. INTRODUCTION

Viscoelastic (VE) dampers (e.g., Figure 1a) are among the effective passive control devices against earthquake and wind-induced structural vibrations. They dissipate the kinetic energy through the shear deformation of the laminated VE slabs, and in the process, heat is generated. Their dynamic mechanical properties (storage stiffness K'_d and loss stiffness K''_d) are commonly determined from the typical force-deformation hysteresis obtained from harmonic loading excitation, as shown in Figure 1b. Here, $K'_d = F'_{d0}/u_{d0}$ and $K''_d = F''_{d0}/u_{d0}$ where F'_{d0} and F''_{d0} = damper forces at peak deformation u_{d0} and zero deformation, respectively. The area enclosed by the ellipse corresponds to the energy dissipated in the respective cycle W_d .

Moreover, VE dampers are known to be highly dependent on the temperature and excitation frequency. As such, their K'_d and K''_d tend to decrease when they are subjected to long-duration loading, due to significant amount of heat generated and stored.

Previous studies such as those by Gopalakrishna and Lai [1], Kasai *et al.* [2], De Casenove *et al.* [3], and Guo *et al.* [4] proposed different thermal-mechanical models for the analysis of VE dampers. These models predicted accurately the temperature-rise and the subsequent property decrement of tested VE dampers.

However, the previous studies above did not investigate the characteristics of the heat flow was not investigated. Hence, this current paper investigates the heats generated, conducted, stored and dispersed by using the three-dimensional finite-element (3D-FE) method of Kasai *et al.* [2]. This investigation further led to the characterization of the global behavior of VE damper.

2. VE DAMPER UNDER LONG-DURATION LOADING

2.1 Damper Specimen and Loading Conditions

This study utilizes the VE damper tested in the Kasai *et al.* [2] study. Figure 1 depicts the basic configuration of the said VE damper that was subjected to harmonic loading with $\pm 50\%$ peak shear strain at 0.333 Hz. Total duration of loading is 3,000 seconds (1,000 cycles). During the test, the ambient temperature was at 24 °C. Note: For more details, please see Reference [2].

2.2 The Three-Dimensional Finite-Element (3D-FE) Method

The 3D-FE method proposed by Kasai *et al.* [2] was used to analyze the VE damper specimen. This method couples the 3D static analysis and transient- and steady-state heat transfer analyses. For an overview, the said method estimates cycle-by-cycle the storage shear

modulus G'_j and the loss factor η_j of each 3D element j of the VE slab at the beginning of the cycle for static analysis as:

$$G'_j = G \frac{1+a_j b_j \omega^{2\alpha} + (a_j + b_j) \omega^\alpha \cos(\alpha\pi/2)}{1+a_j^2 \omega^{2\alpha} + 2a_j \omega^\alpha \cos(\alpha\pi/2)}, \text{ and} \quad (1a)$$

$$\eta_j = \frac{(-a_j + b_j) \omega^\alpha \sin(\alpha\pi/2)}{1+a_j b_j \omega^{2\alpha} + (a_j + b_j) \omega^\alpha \cos(\alpha\pi/2)}. \quad (1b)$$

Here, α = fractional derivative order, G = static shear modulus, ω = circular frequency (rad/s), and a_j and b_j = parameters of the fractional derivative dependent of temperature θ_j at the beginning of the corresponding cycle calculated as:

$$a_j = a_{ref} \lambda_j^\alpha, \quad b_j = b_{ref} \lambda_j^\alpha, \quad \text{and} \quad \lambda_j = \exp \frac{-p_1(\theta_j - \theta_{ref})}{p_2 + \theta_j - \theta_{ref}}. \quad (2a-c)$$

Here, λ_j = corresponding shift factor, a_{ref} and b_{ref} = values of a and b at reference temperature θ_{ref} , respectively.

The energy dissipated per cycle W_j by each element j can be approximated similarly as Figure 1b, and the heat generation rate per unit volume \dot{W}_j in the corresponding cycle of period T can be calculated as:

$$W_j \approx \pi \eta_j G_j^2 \gamma_{xx,j}^2 V_j, \quad \text{and} \quad \dot{W}_j = W_j / (V_j T), \quad (3a, b)$$

respectively. Here, $\gamma_{xx,j}$ and $V_j = ZX$ shear strain and volume of the 3D element j , respectively.

Moreover, the K'_d and K''_d from the 3D static analysis for the corresponding cycle can be approximated as:

$$K'_d = F'_d / u_{d0}, \quad \text{and} \quad K''_d = (\sum_j W_j) / (\pi u_{d0}^2). \quad (4a, b)$$

Due to page limitations, the remaining details of the method are not provided. Please see Reference [2] for more details.

2.3 Analysis Results

In analyzing the VE damper specimen using 3D-FE method, this study used heat transfer coefficient $a_c = 0.28$ N/s/cm²/°C for all air-exposed surfaces. Since the VE damper is symmetrical in the XY-plane (Figure 1a), only half was modeled for analysis. Analysis was carried out using ABAQUS along with a FORTRAN subroutine to amend the VE properties after each loading cycle.

Figure 2 shows the temperature distribution at $t = 2997.75$ seconds, where most of the heat is accumulated within the VE slab. From initial temperature of 24 °C, the VE slab reached a maximum temperature of 28.93 °C at the end of the loading duration. Moreover,

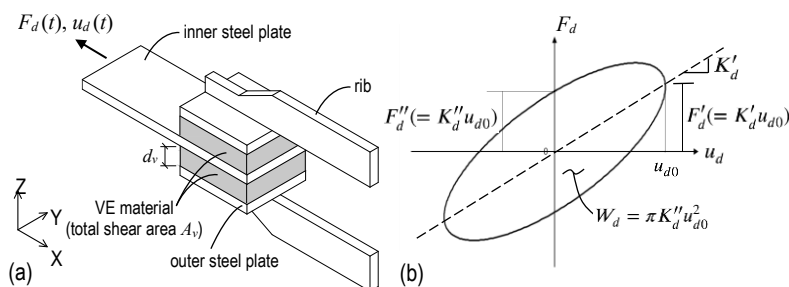


Figure 1. (a) Example of a viscoelastic damper, and (b) force-deformation hysteresis.

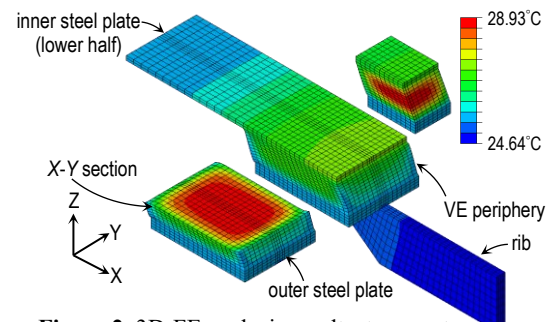


Figure 2. 3D-FE analysis results: temperature distribution at $t = 2997.75$ seconds.

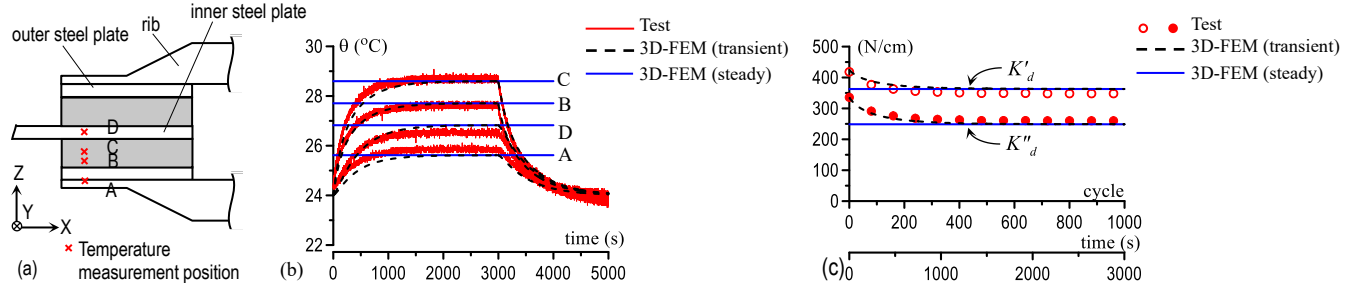


Figure 3. (a) Locations of thermocouples, and (b) temperatures at measurement points and (c) stiffnesses K'_d and K''_d : test vs. analysis.

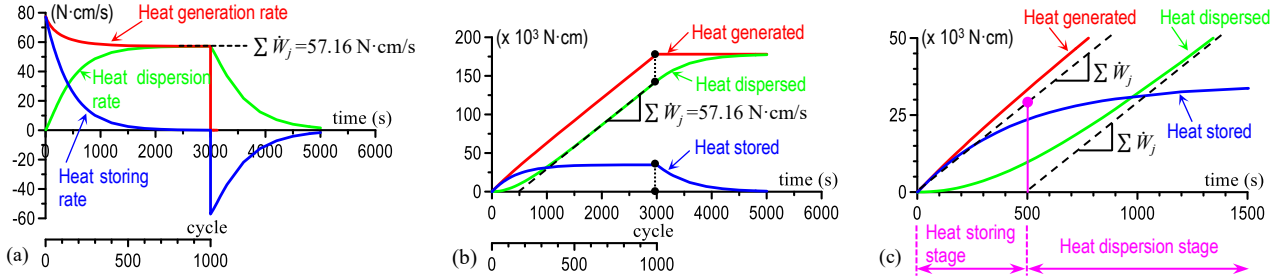


Figure 4. Heat flow characteristics: (a) heat generation rate, heat dispersion rate, and heat storing rate, (b) amounts of heat generated, heat dispersed, and heat stored, and (c) definition of heat storing stage and heat dispersion stage.

Figure 3b shows good agreement between the temperatures from the 3D-FE analysis and the experimentally measured temperatures at different locations (Figure 3a).

As for the global behavior, Figure 3c shows an accurate K'_d and K''_d predictions in the transient and the steady states. The decreasing and the stable values of the K'_d and K''_d during the application of harmonic loading are attributed to increasing and stable damper temperatures (Figure 3b), respectively.

3. HEAT FLOW CHARACTERISTICS

Figure 4a shows that the heat generation rate slows down to a steady value of $57.16 \text{ N}\cdot\text{cm/s}$. Meanwhile, the heat dispersion rate increases and converges with heat generation rate. At such convergence, thermal equilibrium is reached where no additional heat is being stored, and that the VE damper behaves in steady-state manner. Note: Heat storing rate is the difference between the heat generation rate and heat dispersion rate.

After application of harmonic loading, the heat generation rate becomes zero, and the heat stored within the damper is dispersed to the surrounding air, thus, the negative heat storing rate.

Integrating the above quantities with respect to time gives the accumulation of heats generated, dispersed and stored, as shown in Figure 4b. The heat generated and heat dispersed exhibits parallel lines, thereby, we adopt bilinear approximation and define the transient and steady states as *heat storing stage* and *heat dispersion stage*, respectively. The transition time between the two stages is determined by drawing a line of slope $= \Sigma \dot{W}_j$ at the end of loading. As in Figure 4c, the transition time is defined by the point of intersection with horizontal axis at about $t = 500 \text{ s}$ (Cycle 167).

By this approximation, significant heat storing occurs during the transient state until the transition time, and heat dispersion occurs only after the transition time. Although this is a crude idealization, it matches well with the hysteretic behavior.

About half of the heat stored is in VE slab, i.e., approximately $14.3 \text{ N}\cdot\text{cm}$ ($= \Sigma \dot{W}_j \times 500 \text{ s} \times 0.5$). Dividing it by $(sp_{VE}) = 194 \text{ N/cm}^2/^\circ\text{C}$ and volume 25.5 cm^3 (one VE slab) gives $2.59 \text{ }^\circ\text{C}$. From this, the average temperature within the VE slab at $t = 500 \text{ s}$ is $26.59 \text{ }^\circ\text{C}$, and substituting it into Equations 2 and 1, we obtain $G' = 12.91 \text{ N/cm}^2$. Converting it, $K'_d = 371 \text{ N/cm}$ which is 0.99 times the steady-state value predicted by the 3D-FE method (Figure 3c). This provides an

understanding and estimation of average temperature-rise in the VE slab as well as corresponding VE material properties by using Figure 4c and hand calculation.

4. CONCLUSION

This paper characterizes the global behavior of VE damper subjected to long-duration loading by using three-dimensional finite-element (3D-FE) method that couples 3D static analysis and transient- and steady-state heat transfer analyses.

In the transient state, significant heat storing occurs until the transition time. About half of the heat stored is in the VE slabs while the remaining half is in the steel assembly. This reveals that the heat generated within the VE slab is conducted and stored in the adjacent steel assembly.

After the transition time, the VE damper behaves in steady state wherein significant heat dispersion occurs.

A bilinear approximation of VE damper global behavior based on the above heat flow characteristics was carried out. Hand calculation gave a matching result with those from the 3D-FE analysis.

Moreover, this study demonstrated the vital role of the steel material in, not only heat dispersion, but also heat storing that greatly influences the transient-state behavior of VE damper.

ACKNOWLEDGEMENT

This work was supported by JST Program on Open Innovation Platform with Enterprises, Research Institute and Academia.

REFERENCES

- [1] Gopalakrishna H.S., Lai M.L. Finite Element Heat Transfer Analysis of Viscoelastic Damper for Wind Applications. *J. Wind Eng. Ind. Aerod.*, 1998;77&78:283-295.
- [2] Kasai K., Sato D., and Huang Y.H. Analytical Methods for Viscoelastic Damper considering Heat Generation, Conduction, and Transfer under Long Duration Cyclic Load, *Journal on Structural and Construction Engineering* (Transactions of AIJ) No.566, 61-69, Jan. 2006 (In Japanese)
- [3] De Cazenove J., Rade D.A., De Lima A.M.G., Araujo C.A. A Numerical and Experimental Investigation on Self-Heating Effects in Viscoelastic Dampers. *Mechanical Systems and Signal Processing*, 2012;27:433-445.
- [4] Guo, J.W.W., Daniel Y., Montgomery M., Christopoulos C. Thermal mechanical model for the prediction of wind and seismic response of viscoelastic dampers. *J. Eng. Mech.* 2016;142 (10): 04016067.

*1 東京工業大学 博士研究 Ph.D. (元大学院生)

*2 東京工業大学 教授 Ph.D.

*3 東京工業大学 准教授・博士 (工学)

*1 Postdoctoral Fellow, Tokyo Institute of Technology, Ph.D. (Former graduate student)

*2 Professor, Tokyo Institute of Technology, Ph.D.

*3 Assoc. Prof., Tokyo Institute of Technology, D.Eng.